Archives of Materials Science and Engineering

Volume 51
Issue 1
September 2011
Pages 40-47

International Scientific Journal
published monthly by the
World Academy of Materials
and Manufacturing Engineering

Structure and adhesion of thin coatings deposited by PVD technology on the X6CrNiMoTi17-12-2 and X40CrMoV5-1 steel substrates

K. Lukaszkowicz [a,*], A. Kriz [b], J. Sondor [c]

[a] Division of Materials Processing Technology, Management and Computer Techniques in Materials Science, Institute of Engineering Materials and Biomaterials, Silesian University of Technology, ul. Konarskiego 18a, 44-100 Gliwice, Poland

[b] Faculty of Materials Science and Metallurgy, University of West Bohemia, Univerzitni 8, 306 14 Plzen, Czech Republic

[c] LISS, a.s., Zuberska 2603, 756-61 Roznov p.R., Czech Republic

* Corresponding author: E-mail address: krzysztof.lukaszkowicz@polsl.pl

Received 18.06.2011; published in revised form 01.09.2011

ABSTRACT

Purpose: The main aim of the research was the investigation of the structure and adhesion of AlTiCrN, CrAlSiN and TiAlSiN coatings deposited by physical vapour deposition technology on the X40CrMoV5-1 hot work tool steel and the X6CrNiMoTi17-12-2 austenitic stainless steel substrate.

Design/methodology/approach: Observations of surface and microstructure of the deposited coatings were carried out on cross sections in the SUPRA 35 scanning electron microscope. The microhardness tests of coatings were made with the SHIMADZU DUH 202 ultra-microhardness tester. The cohesion and adhesion properties of the coatings were made using the scratch test on the CSEM REVETEST device.

Findings: It was found that the coatings present a compact structure, without any visible delaminations or defects. The morphology of the fracture of coatings is characterized by a dense structure, in some cases there is a columnar structure. The coatings demonstrated good adhesion to the substrate. The critical load L_{C2} lies within the range of 39-47 N, depending on the coating and substrate type. The coatings demonstrate a high hardness (~40 GPa).

Practical implications: The process of covering steels with the thin PVD coatings is currently the most commonly method used to extend their life. Investigations of those coatings determining their scratch-resistant properties and structure enable to pick out the optimum coatings for given industrial applications.

Originality/value: The results of the investigation provide useful information on microstructure and scratch-resistant properties of the quaternary coatings deposited on the hot work tool steels and austenitic stainless steels.

Keywords: Thin and thick coatings; PVD; Adhesion; Microstructure

Reference to this paper should be given in the following way:

K. Lukaszkowicz, A. Kriz, J. Sondor, Structure and adhesion of thin coatings deposited by PVD technology on the X6CrNiMoTi17-12-2 and X40CrMoV5-1 steel substrates, Archives of Materials Science and Engineering 51/1 (2011) 40-47.

PROPERTIES

1. Introduction

Fast development of the PVD processes has offered the potential of the specific coatings properties on an industrial scale [1-6]. Analysing properties of coatings developed in the PVD processes one has to pay special attention to issues connected with their mechanical properties (adhesion, hardness, internal stresses, etc.), physical properties, abrasive wear resistance, corrosion, diffusion-, and thermal protection, structure, chemical composition and thickness of the coatings [7-12]. Adhesion of the coating to the substrate features one of the key issues pertaining to coating items with the hard ceramic materials. Therefore, it is one of the most important properties of coatings deposited by PVD processes. Should the adhesion be inappropriate, then the entire coating functionality may be lost. Therefore, the coating-substrate contact zone is important when the reliable and durable coating is to be worked out. The employment of a thin intermediate layer, e.g. the Ti one, improves adhesion of the true coating, as the soft titanium layer reduces stresses and counteracts propagation of cracks. Because of the technological issues and reliability of the coating-substrate system, high hardness and good adhesion of the coating to the substrate should always be the first requirements to be taken into consideration [13-16].

In recent fifteen years, quaternary coatings (TiAlSiN, CrAlSiN, AlTiCrN, etc.) have been a subject of interest both for scientific research and for industrial application. In comparison with the earlier developed coatings, the quaternary coatings often combine the individual advantages of these coatings and have high hardness, wear resistance and good adhesion to substrate [17-19]. Different techniques are available for the preparation of quaternary coatings. The most promising methods are plasma assisted chemical vapour deposition (PACVD) or PVD vacuum arc evaporation technology.

The advantages of deposition of coatings by means of vacuum arc are the high deposition rate and fully ionized plasma. Nowadays one of the commonly used coating equipment for large-scale industrial production is the LARC® Technology. The most important advantages on the LARC® Technology come from the rotating cathodes and their lateral position.

The purpose of this paper is to examine the structure and adhesion of AlTiCrN, CrAlSiN and TiAlSiN coatings deposited by physical vapour deposition technology on the X40CrMoV5-1 hot work tool steel and the X6CrNiMoTi17-12-2 austenitic stainless steel substrate.

2. Investigation methodology

The tests were made on specimens of the X40CrMoV5-1 hot work tool steel and the X6CrNiMoTi17-12-2 austenitic stainless steel deposited with TiAlSiN, CrAlSiN and AlTiCrN thin coatings.

To ensure proper quality, the surfaces of the cylindrical steel specimens (30×5 mm) were subjected to mechanical grinding and polishing (R_a = 0.03 μm). The specimens were cleaned in an ultrasonic bath with alcohol. Immediately after the cleaning procedure, the samples were placed into the vacuum chamber. Finally, the samples were sputter-cleaned in argon plasma and a thin metallic Ti layer was deposited on the substrates prior to the coatings.

The coatings were deposited in the arc plating Physical Vapour Deposition unit PLATIT® π80, LAteral Rotating ARC-Cathodes (LARC) technology. Coatings` deposition was carried on in an Ar and N_2 atmosphere. Cathodes containing pure metals (Cr, Ti) and AlSi (88:12 wt.%), TiAl (50:50 at.%), AlTi (67:33 at.%) alloys were used for coatings deposition. The base pressure in the vacuum chamber was 5×10^{-4} Pa. The deposition conditions are summarized in Table 1.

Table 1.
Deposition parameters of the coatings

Coating	Substrate bias voltage, V	Arc current source, A	Pressure, Pa	Temperature, °C
TiAlSiN	-90	Ti – 80 AlSi – 120	2.0	450
CrAlSiN	-60	Cr – 70 AlSi – 120	3.0	450
AlTiCrN	-60	Cr – 70 AlTi – 120	2.0	450

Table 2.
Description of critical loads corresponding to different failure modes [14]

Critical load	Description of failure mode
L_{C1}	The first cohesion-related failure event; the first appearance of micro cracking, surface flaking inside/outside the track without any exposure of the substrate
L_{C2}	The first adhesion-related failure event: the first appearance of cracking, chipping, spallation and delamination inside/outside the track with the exposure of the substrate
L_{C3}	The first breakthrough: the first exposure of the substrate in the scratch track resulting from wear
L_S	Coating worn out in the track

Observations of surface and structures of the deposited coatings were carried out on cross sections in the SUPRA 35 scanning electron microscope. Detection of secondary electron was used for generation of fracture images with 20-kV bias voltage.

The microhardness tests of coatings were made with the SHIMADZU DUH 202 ultra-microhardness tester. The test conditions were selected so as to obtain comparable test results for all coatings. Measurements were made at 0.05 N load, to eliminate the substrate impact on the coating hardness.

The cohesion and adhesion properties of the coatings were made using the scratch test on the CSM REVETEST device, by moving the diamond indenter along the examined specimen's surface with gradually increasing load. The radius of the diamond indenter used in the scratch test was 200 μm. The device registered the friction force, friction coefficient, indenter penetration depth and acoustic emission along the scratch track. The tests were made using the following parameters:

- load range: 0-100 N,
- load increase rate (dL/dt): 100 N/min,
- indenter's sliding speed (dx/dt): 10 mm/min,
- acoustic emission detector's sensitivity AE: 1.

The critical loads were determined on the basis of the values of the acoustic emission AE and friction force Ft recorded and observation of the damage developed in the scratch test on a LEICA MEF4A light microscope. The critical loads corresponding to the failure modes as defined in Table 2.

The thickness of coatings was determined using the ''kalotest'' method, i.e. measuring the characteristics of the spherical cap crater developed on the surface of the coated specimen tested.

3. Discussion of results

The coatings present a compact structure, without any visible delaminations or defects. The morphology of the fracture of coatings is characterized by a dense structure, in some cases there is a columnar structure (Figs. 1, 2). The fracture surface of the steel samples was examined and the deposited coatings show a sharp transition zone between the substrate and the coating.

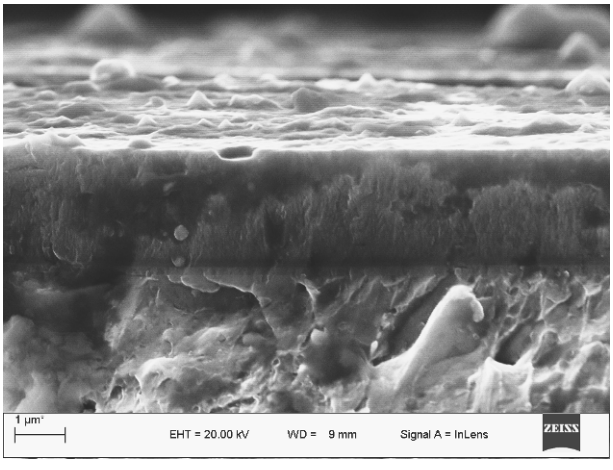

Fig. 1. Fracture of the CrAlSiN coating on the X40CrMoV5-1 hot work tool steel substrate

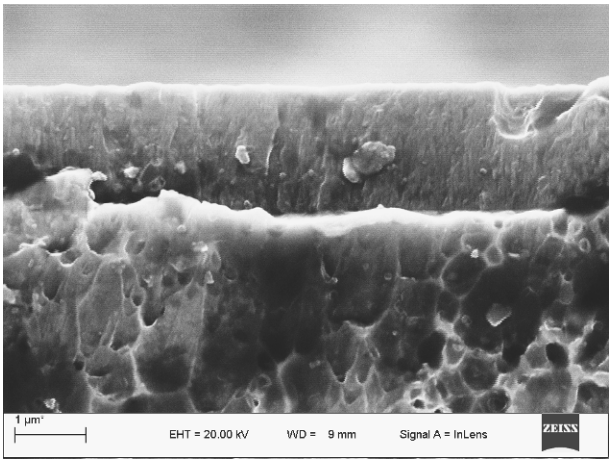

Fig. 2. Fracture of the TiAlSiN coating on the X40CrMoV5-1 hot work tool steel substrate

The morphology of the coatings' surface is characteristic of microdroplets (Fig. 3), which are a well-known drawback of the cathodic arc evaporation. Examinations of the chemical composition of these droplets demonstrated that they developed from pure metals. This leads to the conclusion that they were ejected from boiling liquid metal in the cathode spots on the target`s surface and solidified on the substrate surface. The size of these particles changes from several tenths of 1 μm to about 2 μm.

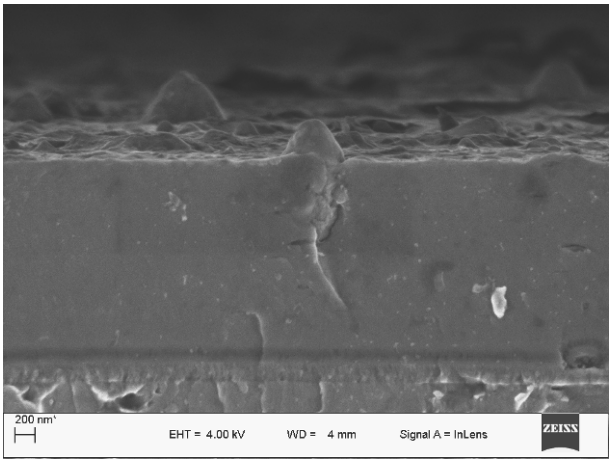

Fig. 3. Topography of the CrAlSiN coating on the X40CrMoV5-1 hot work tool steel substrate

The hardness of the coatings tested fits within the range from 40 to 42 GPa. The highest hardness was recorded in the case of the AlTiCrN coating (Table 3).

Coating thickness (Table 3) measurements made on fractures in the scanning electron microscope and confirmed by measurements made with the "kalotest" method (Fig. 4) revealed that their values are within the range 2.1-3.0 μm, depending on the coating type, as well as time and parameters of the coating deposition process.

The critical load values were determined using the scratch method with the linearly increasing load („scratch test"), characterizing adherence of the investigated coatings to the austenitic stainless steel and hot work tool steel substrate. The investigated coatings shows relatively low values of critical load. First failure occurs at very low values (~ 10 N). In case of the coatings examined, it was found that coating AlTiCrN had the highest critical load value L_S=47 N deposited on substrate made of the X40CrMoV5-1 steel, while CrAlSiN and TiAlSiN coatings deposited on the substrate made of the X6CrNiMoTi17-12-2 steel – had the lowest value. In general, the coatings deposited on the substrate made of the X40CrMoV5-1 hot work tool steel show better adherence to the substrate than coatings deposited on the substrate made of the X6CrNiMoTi17-12-2 austenitic steel. This is caused by a significantly higher hardness of the X40CrMoV5-1 steel.

The critical loads recorded during the scratch test are dependent not only on the mechanical strength (adhesion, cohesion) of the coating/substrate system, but also on various parameters connected with the coating/substrate system (substrate hardness and roughness, coating hardness and roughness, coating thickness, friction coefficient between the coating and the indenter, internal stresses in coatings), and also on the test parameters alone (load increase rate, indenter feed, curvature radius of the indenter's tip, indenter's material, and indenter's tip wear).

In order to establish the nature of damage, the cracks produced during the test were examined by the light microscope coupled with the measuring device, determining the critical loads in virtue of metallographic observations.

During the adhesion investigation using the scratch test, defects develop, which P.J. Burnett et al. [20] classified as follows:

- spalling failure;
- buckling failure;
- chipping failure;
- conformal craking;
- tensile craking.

In case of AlTiCrN coatings the first symptoms of damage of the coatings examined are conformal or tensile microcracking indicating cohesive failure within the investigated coatings, as a results of substrate deformation (Figs. 5-8). Occasionally, there are some small chippings on the scratch edges. With the load increase, buckling failure (X6CrNiMoTi17-12-2) or chipping failure (X40CrMoV5-1) along the scratch track borders occurs.

Table 3.
The characteristics of the tested coatings

Coating	Microhardness, GPa	Thickness, µm		Critical load L_{C1}, N		Critical load L_{C2}, N		Critical load L_{C3}, N		Critical load L_S, N	
		ASS	HWTS	ASS	HWTS	ASS	HWTS	ASS	HWTS	ASS	HWTS
AlTiCrN	42	2.3	2.4	10±0	29±4	19±0	31±2	32±6	40±7	36±3	47±5
CrAlSiN	40	3.0	2.9	9±1	17±1	12±1	21±0	28±1	41±6	34±1	45±5
TiAlSiN	40	2.1	2.2	6±0	13±1	11±0	17±1	21±1	36±1	35±2	39±1

ASS – austenitic stainless steel, HWTS – hot work tool steel

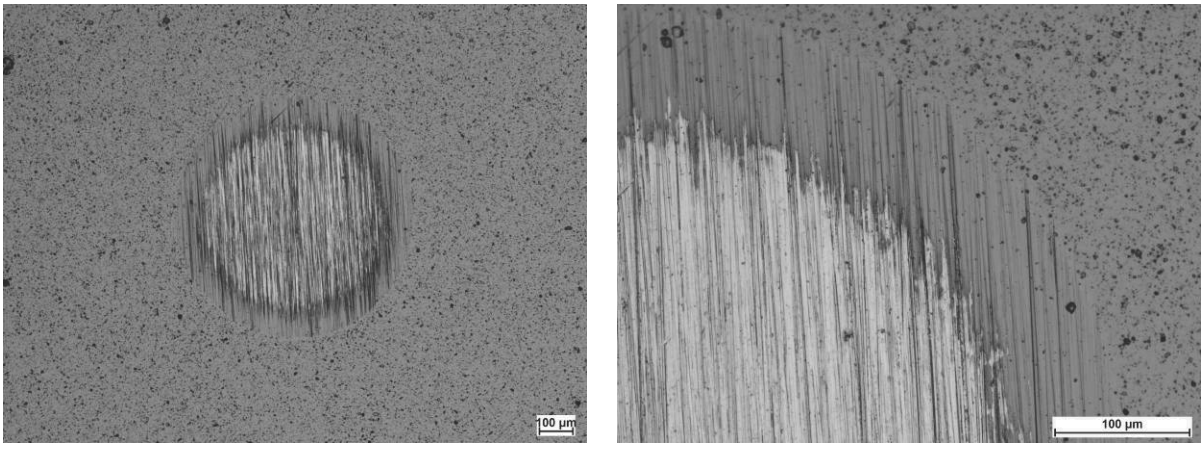

Fig. 4. Kalotest crater performed on the AlTiCrN coating deposited on the X6CrNiMoTi17-12-2 austenitic stainless steel substrate

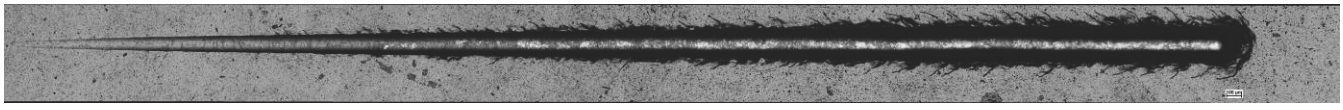

Fig. 5. Optical micrographs of scratch paths in the AlTiCrN coating deposited on the X6CrNiMoTi17-12-2 austenitic stainless steel substrate

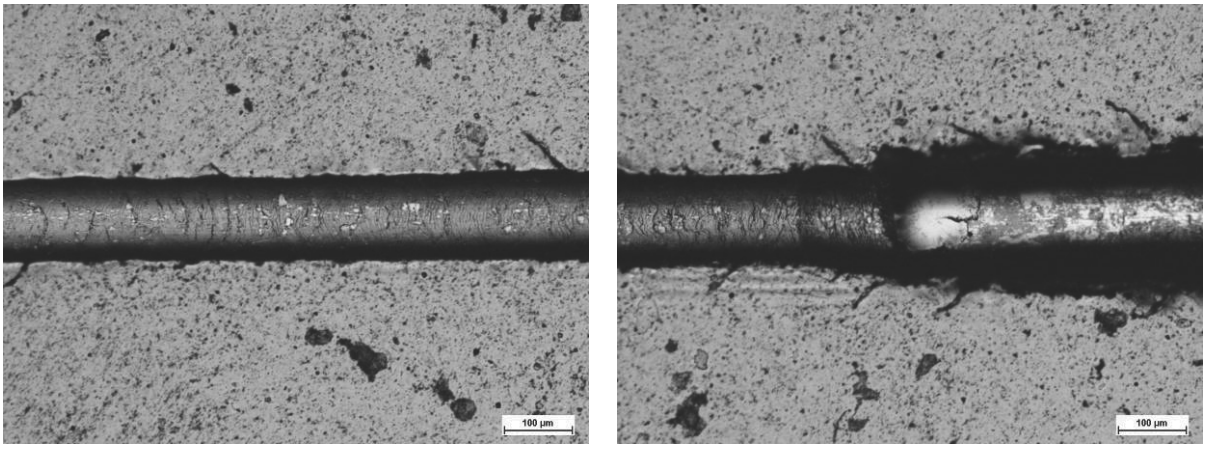

Fig. 6. Main part of a scratch track in the AlTiCrN coating deposited on the X6CrNiMoTi17-12-2 austenitic stainless steel substrate

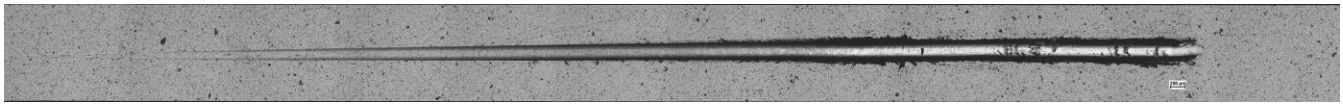

Fig. 7. Optical micrographs of scratch paths in the AlTiCrN coating deposited on the X40CrMoV5-1 hot work tool steel substrate

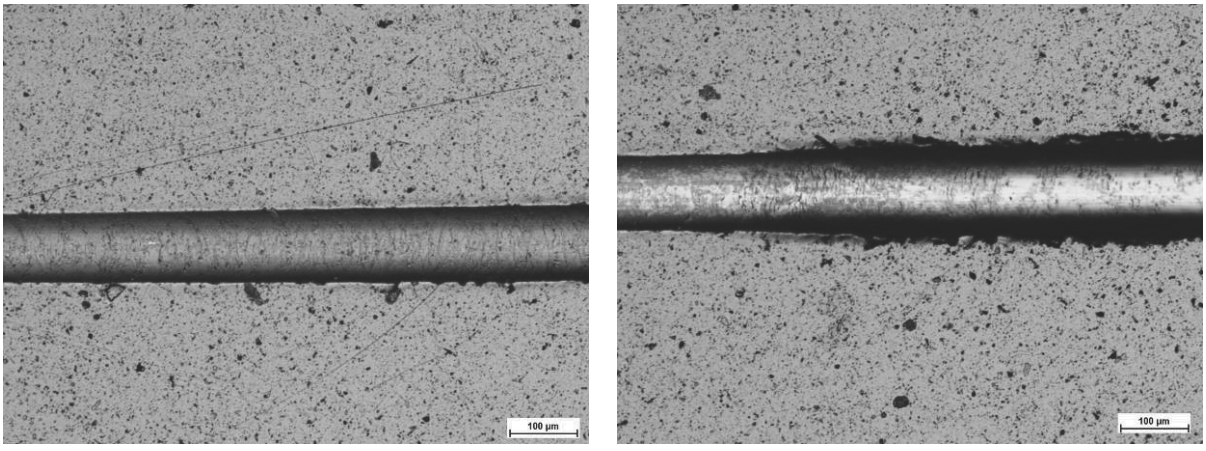

Fig. 8. Main part of a scratch track in the AlTiCrN coating deposited on the X40CrMoV5-1 hot work tool steel substrate

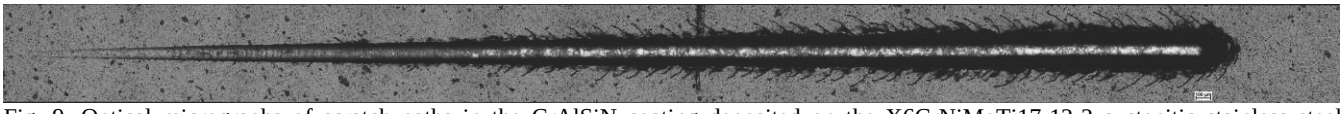

Fig. 9. Optical micrographs of scratch paths in the CrAlSiN coating deposited on the X6CrNiMoTi17-12-2 austenitic stainless steel substrate

In case of CrAlSiN coatings the first symptoms of damage of the coatings examined are conformal cracking indicating cohesive failure within the investigated coatings, as a results of substrate deformation (Figs. 9-12). Occasionally, there are some small chippings on the scratch edges. With the load increase, buckling failure (X6CrNiMoTi17-12-2) or recovery spallation (X40CrMoV5-1) along the scratch track borders occurs.

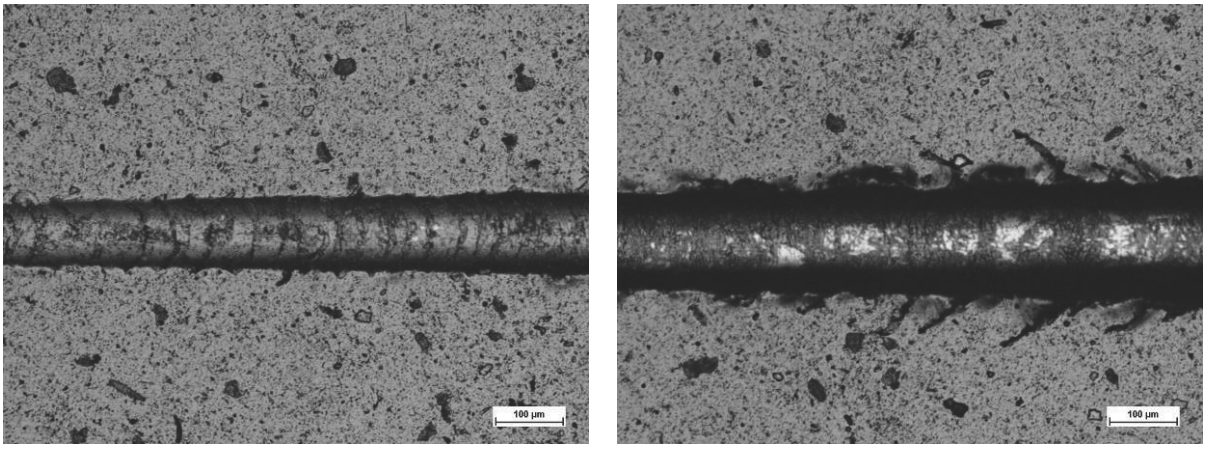

Fig. 10. Main part of a scratch track in the CrAlSiN coating deposited on the X6CrNiMoTi17-12-2 austenitic stainless steel substrate

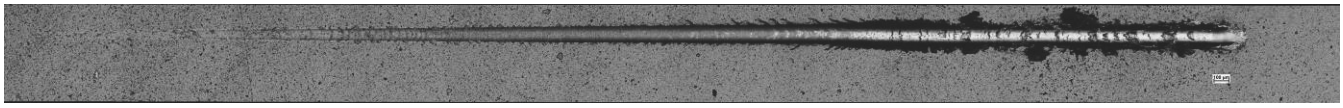

Fig. 11. Optical micrographs of scratch paths in the CrAlSiN coating deposited on the X40CrMoV5-1 hot work tool steel substrate

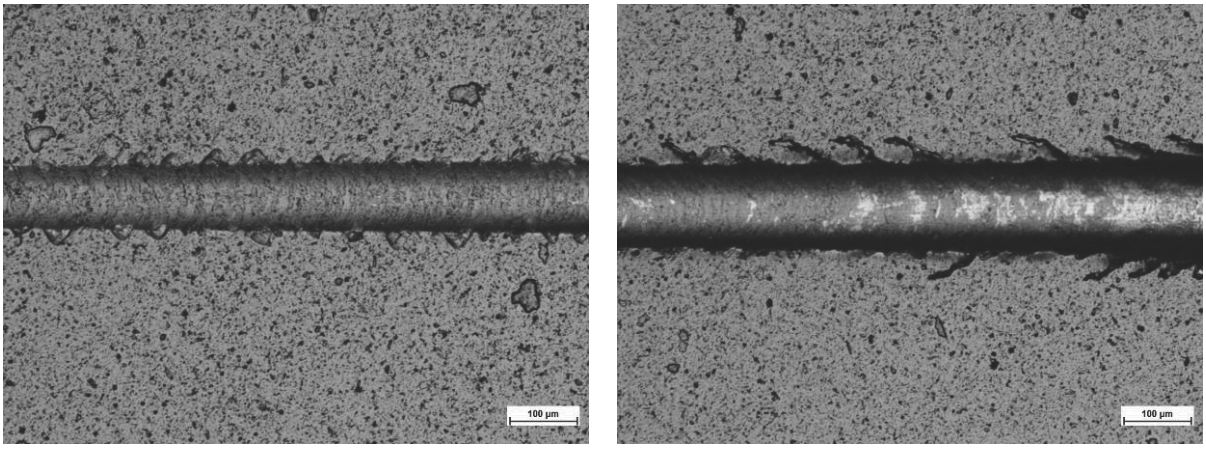

Fig. 12. Main part of a scratch track in the CrAlSiN coating deposited on the X40CrMoV5-1 hot work tool steel substrate

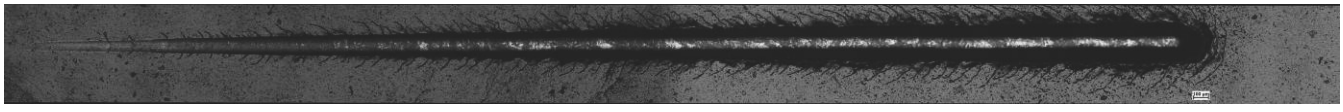

Fig. 13. Optical micrographs of scratch paths in the TiAlSiN coating deposited on the X6CrNiMoTi17-12-2 austenitic stainless steel substrate

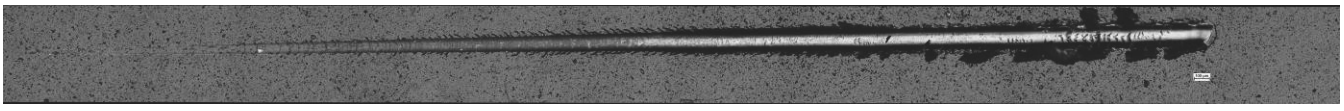

Fig. 14. Optical micrographs of scratch paths in the TiAlSiN coating deposited on the X40CrMoV5-1 hot work tool steel substrate

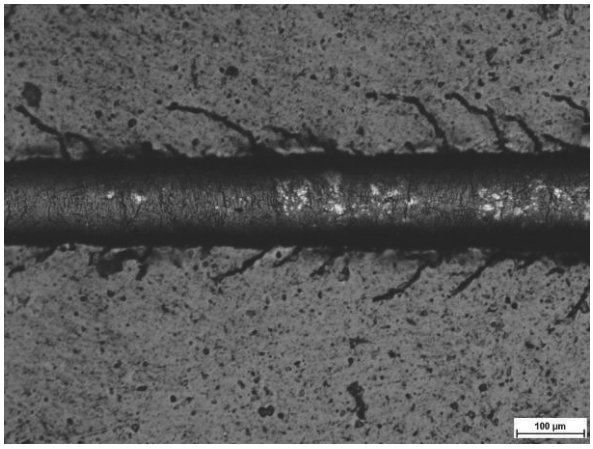

Fig. 15. Main part of a scratch track in the TiAlSiN coating deposited on the X6CrNiMoTi17-12-2 austenitic stainless steel substrate

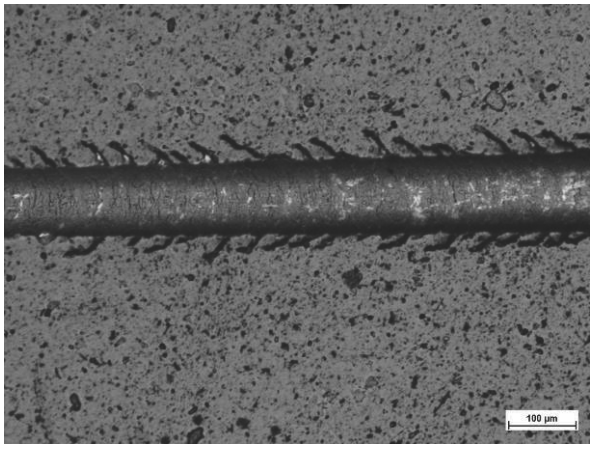

Fig. 16. Main part of a scratch track in the TiAlSiN coating deposited on the X40CrMoV5-1 hot work tool steel substrate

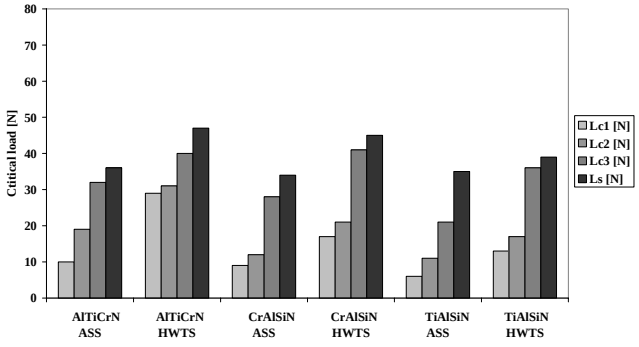

Fig. 17. A summary of the critical load (scratch test) for the investigated coatings deposited on the X6CrNiMoTi17-12-2 austenitic stainless steel (ASS) and X40CrMoV5-1 hot work tool steel (HWTS) substrate

In case of TiAlSiN coatings the first symptoms of damage of the coatings examined are conformal cracking indicating cohesive failure within the investigated coatings, as a results of substrate deformation (Figs. 13-16). Occasionally, there are some small chippings on the scratch edges. With the load increase, buckling and chipping failure on both sides (X6CrNiMoTi17-12-2) or recovery spallation (X40CrMoV5-1) along the scratch track borders occurs.

The critical load values shown in Figure 17 are summarized in Table 3.

4. Summary

The compact structure of the coatings without any visible delaminations was observed as a result of tests in the scanning electron microscope. The fracture morphology of the coatings tested is characterised with a dense and columnar structure.

The coating adhesion scratch tests disclose the cohesion and adhesion properties of the coatings tested. In virtue of the tests carried out, it was found that the critical load L_S fitted within the range 39-47 N for the coatings deposited on a substrate made of hot work tool steel X40CrMoV5-1 and 34-36 N for coatings deposited on the substrate made of the X6CrNiMoTi17-12-2 austenitic stainless steel. The coatings deposited on the substrate made of the X40CrMoV5-1 steel present a better adhesion than the coatings deposited on the substrate made of the X6CrNiMoTi17-12-2 steel.

Acknowledgements

Research was financed in a part within the framework of the Polish State Committee for Scientific Research Project No N N507 550738 headed by Krzysztof Lukaszkowicz, Ph.D., Eng. and within the framework of the Scholarship No 51100929 of the International Visegrad Fund realized by Krzysztof Lukaszkowicz, Ph.D., Eng.

References

[1] K. Lukaszkowicz, L.A. Dobrzański, A. Zarychta, Structure, chemical and phase compositions of coatings deposited by reactive magnetron sputtering onto the brass substrate, Journal of Materials Processing Technology 157-158 (2004) 380-387.

[2] L.A. Dobrzański, K. Lukaszkowicz, A. Kriz, Properties of the multi-layer Ti/CrN and Ti/TiAlN coatings deposited with the PVD technique onto the brass substrate, Journal of Materials Processing Technology 143-144 (2003) 832-837.

[3] D. Pakuła, L.A. Dobrzański, K. Gołombek, M. Pancielejko, A. Křiž, Structure and properties of the Si_3N_4 nitride ceramics with hard wear resistant coatings, Journal of Materials Processing Technology 157-158 (2004) 388-393.

[4] D. Pakuła, L.A. Dobrzański, A. Križ, M. Staszuk, Investigation of PVD coatings deposited on the Si_3N_4 and

sialon tool ceramics, Archives of Materials Science and Engineering 46/1 (2010) 53-60.
[5] L.A. Dobrzański, M. Staszuk, J. Konieczny, W. Kwaśny, M. Pawlyta, Structure of TiBN coatings deposited onto cemented carbides and sialon tool ceramics, Archives of Materials Science and Engineering 38/1 (2009) 48-54.
[6] K. Lukaszkowicz, J. Szewczenko, M. Pancielejko, Structure, mechanical properties and corrosion resistance of PVD gradient coatings deposited onto the X40CrMoV5-1 hot work tool steel substrate, International Journal of Materials and Product Technology 39 (2010) 148-158.
[7] L.A. Dobrzański, K. Lukaszkowicz, K. Labisz, Structure, texture and chemical composition of coatings deposited by PVD techniques, Archives of Materials Science and Engineering 37/1 (2009) 45-52.
[8] L.A. Dobrzanski, K. Lukaszkowicz, Erosion resistance and tribological properties of coatings deposited by reactive magnetron sputtering method onto the brass substrate, Journal of Materials Processing Technology 157-158 (2004) 317-323.
[9] L.A. Dobrzański, D. Pakuła, Structure and properties of the wear resistant coatings obtained in the PVD and CVD processes on tool ceramics, Materials Science Forum 513 (2006) 119-133.
[10] M. Drak, L.A. Dobrzański, Corrosion of Nd-Fe-B permanent magnets, Journal of Achievements in Materials and Manufacturing Engineering 20 (2007) 239-241.
[11] L.A. Dobrzański, D. Pakuła, Comparison of the structure and properties of the PVD and CVD coatings deposited on nitride tool ceramics, Journal of Materials Processing Technology 164-165 (2005) 832-842.
[12] L.A. Dobrzański, D. Pakuła, A. Křiž, M. Soković, J. Kopač, Tribological properties of the PVD and CVD coatings deposited onto the nitride tool ceramics, Journal of Materials Processing Technology 175 (2006) 179-185.
[13] K. Lukaszkowicz, J. Sondor, A. Kriz, M. Pancielejko, Structure, mechanical properties and corrosion resistance of nanocomposite coatings deposited by PVD technology onto the X6CrNiMoTi17-12-2 and X40CrMoV5-1 steel substrates, Journal of Materials Science 45/6 (2010) 1629-1637.
[14] Y. He, I. Apachitei, J. Zhou, T. Walstock, J. Duszczyk, Effect of prior plasma nitriding applied to a hot-work tool steel on the scratch-resistant properties of PACVD TiBN and TiCN coatings, Surface and Coatings Technology 201 (2006) 2534-2539.
[15] S.J. Bull, Failure mode maps in the thin film scratch adhesion test, Tribology International 30/7 (1997) 491-498.
[16] K. Lukaszkowicz, A. Czyżniewski, W. Kwaśny, M. Pancielejko, Structure and mechanical properties of PVD coatings deposited onto the X40CrMoV5-1 hot work tool steel substrate, Vacuum (2011) doi:10.1016/j.vacuum.2011.10.031
[17] S. Veprek, M.J.G. Veprek-Heijman, Industrial applications of superhard nanocomposite coatings, Surface and Coatings Technology 202 (2008) 5063-5073.
[18] J. Soldan, J. Neidhardt, B. Sartory, R. Kaindl, R. Cerstvy, P.H. Mayrhofer, R. Tessadri, P. Polcik, M. Lechthaler, C. Mitterer, Structure-property relations of arc-evaporation Al-Cr-Si-N coatings, Surface and Coatings Technology 202 (2008) 3555-3562.
[19] G.S. Fox-Rabinovich, K. Yamomoto, S.C. Veldhuis, A.I. Kovalev, G.K. Dosbaeva, Tribological adaptability of TiAlCrN PVD coatings under high performance dry machining conditions, Surface and Coatings Technology 200 (2005) 1804-1813.
[20] P. Burnett, D. Rickerby, The relationship between hardness and scratch adhesion, Thin Solid Films 154 (1987) 403-416.